

Propagation-Induced Escape from Adiabatic Following in a Semiconductor

P. A. Harten, A. Knorr,^(a) J. P. Sokoloff,^(b) F. Brown de Colstoun, S. G. Lee, R. Jin, E. M. Wright,
G. Khitrova, H. M. Gibbs, S. W. Koch,^(c) and N. Peyghambarian

Optical Sciences Center, University of Arizona, Tucson, Arizona 85721

(Received 24 April 1992)

Breakup of a below-resonance femtosecond pulse is observed in a room-temperature GaAs/AlGaAs multiple-quantum-well waveguide using cross-correlation techniques. The breakup is due to neither self-induced transparency nor temporal solitons. Instead, calculations based on the coupled semiconductor Maxwell-Bloch equations show that coherent self-phase-modulation during propagation drives the system out of the initial adiabatic following regime into excitation density oscillations and eventually pulse-shape modulations.

PACS numbers: 78.47.+p, 42.50.Hz, 42.50.Md

Coherent pulse propagation, including self-induced transparency and pulse breakup, has been studied extensively in passive atomic media [1-3]. However, such coherent processes have only recently been considered for semiconductors where the phase relaxation times are very rapid [4,5]. Here we report the first experimental and theoretical investigations showing coherent pulse breakup in a semiconductor waveguide for photon energies below the lowest ($1s$) exciton resonance. In this spectral region the optical Stark effect [6] should produce an ultrafast change in the nonlinear refractive index with a response time limited only by the polarization dephasing time. This suggests that optical solitons may be formed in conjunction with the group-velocity dispersion of the semiconductor waveguide system. However, for the femtosecond experiments reported here the input pulses are shorter than the polarization dephasing so that the coherent nature of the light-semiconductor interaction becomes of paramount importance. Coherent propagation is then shown to drive the system out of the initial adiabatic following regime which leads to pulse breakup and prevents soliton formation.

The experiments have been performed with an amplified (1 kHz repetition rate) hybridly mode-locked dye laser. The center wavelength is $\lambda = 870$ nm and the pulse duration is $t_p \approx 100$ fs full width at half maximum (FWHM) before entering the optics used for coupling into the waveguide. The time-bandwidth product $\Delta\nu t_p = 0.2$ is indicative of transform-limited pulses with asymmetric temporal shape that has been verified using standard cross-correlation techniques [7]. The waveguide is inserted into one arm of the cross-correlator. The 1.2- μm -thick 100- \AA GaAs/AlGaAs multiple-quantum-well guiding region is sandwiched between AlGaAs layers for vertical confinement with ridges in the top layer for horizontal confinement supporting a single transverse guided mode. The light is polarized in the growth direction which simplifies the problem by allowing only the light-hole excitonic transition.

Figures 1(a) and 1(b) show the experimentally measured cross-correlations of the transmitted pulses for both

low and high intensity, respectively. These results were obtained using a 0.37-mm-long waveguide, and peak intensities of 8.5 GW/cm^2 [Fig. 1(b)] and 0.8 GW/cm^2 [Fig. 1(a)]. The 4.5-ps delay observed upon transmission is the result of group-velocity delay. In comparison to the input pulse the transmitted low-intensity pulse in Fig. 1(a) has a 300 fs FWHM, but does not otherwise show any significant distortion. This temporal spread compared to a 100-fs input pulse can be attributed to linear dispersion mainly in the waveguide coupling optics which stretches the pulse to a 200 fs FWHM even without the waveguide, and the spread inherent in the cross-correlation process using a reference pulse of finite duration. In contrast, pulse breakup is clearly seen in Fig. 1(b) for the high-intensity pulse. The main peak of the transmitted pulse still has approximately a 300 fs FWHM, but now a secondary peak appears on the trail-

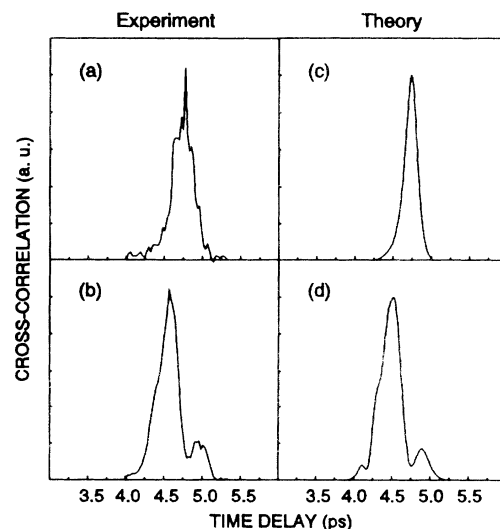


Fig. 1. (a),(b) The measured cross-correlations of transmitted high-intensity and low-intensity femtosecond pulses, respectively. (c),(d) The corresponding calculated cross-correlation pulses with areas of 2π and 7.5π . The time delay zero point is defined by the peak signal without waveguide.

ing edge of the pulse. We also repeated this series of experiments using $t_p = 5$ ps FWHM ($\Delta\nu t_p = 0.31$) input pulses and no breakup was observed even for high intensities.

In order to analyze the experimental results we solve the semiconductor Bloch equations [8] for linearly polarized plane waves traveling in the z direction. The total polarization is written as $P(z, t) = P_b(z, t) + P_{nr}(z, t)$: The first part $P_b(z, t)$ results from the background non-resonant light-matter interaction involving those bands of higher band index than the conduction band, and determines the group velocity, $v_g = (\partial k / \partial \omega)^{-1}$, and the group-velocity dispersion parameter, $k_0'' = \partial^2 k / \partial \omega^2$, both evaluated at the laser frequency $\omega = \omega_0$. The second part $P_{nr}(z, t)$ accounts for the near-resonant interaction between the laser field and conduction and valence bands. After applying the slowly varying envelope approximation for field and polarization the wave equation for pulse propagation in the semiconductor medium is [9]

$$\frac{\partial}{\partial \xi} \bar{E}(\xi, \eta) = -i \frac{\mu_0 \omega_0^2}{2k_0} \bar{P}_{nr}(\xi, \eta) + \frac{i}{2} k_0'' \frac{\partial^2}{\partial \eta^2} \bar{E}(\xi, \eta), \quad (1)$$

where $k_0 = k(\omega_0)$, $\bar{E}(\xi, \eta)$ and $\bar{P}_{nr}(\xi, \eta)$ denote the envelopes of the electric field and the near-resonant part of the polarization, and $(\xi, \eta) = (z, t - z/v_g)$ is the coordinate frame that travels at the group velocity. \bar{P}_{nr} is derived in the two-band approximation neglecting exchange effects since our experiment is performed in the off-resonance low-excitation-density regime for which the k -space electron and hole distributions obey $n_{e,k} + n_{h,k} \ll 1$. The semiconductor Bloch equations then take the form [8]

$$\left(\frac{\partial}{\partial \eta} - i\Delta_\lambda + \frac{1}{\tau} \right) \bar{P}_\lambda(\xi, \eta) = -\frac{i}{2\hbar} (1 - 2n_\lambda) d_{cv} \bar{E}(\xi, \eta), \quad (2)$$

$$\frac{\partial}{\partial \eta} n_\lambda = -\frac{i}{2\hbar} [d_{cv} \bar{P}_\lambda^*(\xi, \eta) \bar{E}(\xi, \eta) - \text{c.c.}]. \quad (3)$$

The energy dispersion of the semiconductor material is contained in $\Delta_\lambda = \omega_\lambda - \omega_0$, where λ labels the discrete exciton energy states as well as the continuum states. Here the excitation density in the λ th state is denoted by n_λ and d_{cv} is the dipole transition moment. The phenomenological polarization dephasing time τ is an approximate average over the dephasing times of the different excitations λ which has provided good agreement between experiment and theory in the case of the optical Stark effect [10]. Because of the extremely short pulses used here we neglect the decay of the excitation densities n_λ . The polarization $\bar{P}_{nr}(\xi, \eta)$ is given by

$$\bar{P}_{nr}(\xi, \eta) = 2 \sum_\lambda d_{cv}^* |\Psi_\lambda(0)|^2 \bar{P}_\lambda(\xi, \eta). \quad (4)$$

The semiconductor Bloch equations (2) and (3), including the polarization (4), and the electromagnetic wave

equation (1), are solved self-consistently for each small slice of material with the initial values $\bar{P}_\lambda(\xi, \eta = -\infty) = 0$ and $n_\lambda(\xi, \eta = -\infty) = 0$. The electric field resulting from the previous step serves as the input field for the next. The asymmetry of the pulse entering the waveguide is included in the model. As a measure of the coherent interaction strength we introduce the pulse area A , defined as the time integral over the Rabi frequency $\Omega(t)$ of the pulse with respect to an intraband electron-hole pair state [1]

$$A = \frac{d_{cv}}{\hbar} \left| \int_{-\infty}^{+\infty} \bar{E}(0, t) dt \right| = \int_{-\infty}^{+\infty} \Omega(t) dt. \quad (5)$$

The numerical values in the calculation are $d_{cv} = 4.8 \times 10^{-29}$ C m, $\tau = 200$ fs, $\hbar \Delta_{1s} = 10 E_R$, where E_R is the bulk exciton Rydberg energy, and $\Delta_{1s} = \omega_{1s} - \omega_0$ is the detuning of the laser frequency from the $1s$ exciton. The maximum input Rabi frequency is $\Omega_0 = 10^{14}$ Hz which corresponds to a pulse of area $A = 7.5\pi$, assuming that the input pulse has slightly spread through the input coupling lens system. The group refractive index $n^* = 4.6$ is measured in our experiment and is consistent with a group index measurement in GaAs double heterostructure lasers at similar detuning from the band edge [11]. The total group-velocity dispersion simulating the waveguide and the output coupling lens system spreads the incident pulse by a factor of 1.33 under linear propagation.

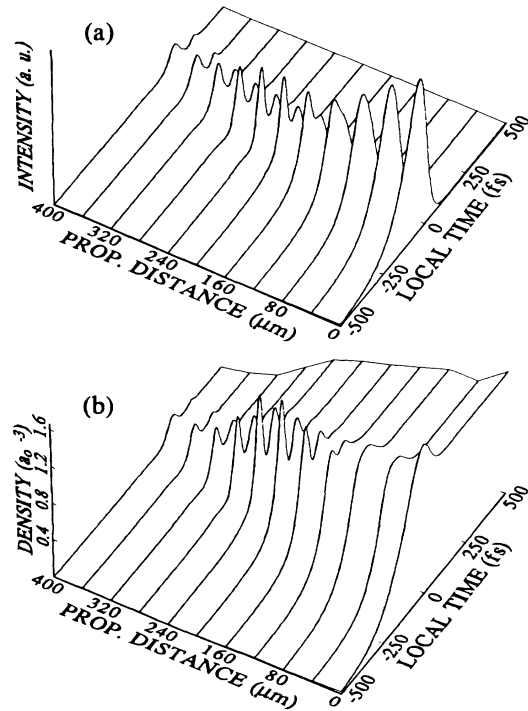


FIG. 2. (a) Calculated temporal profiles of the 7.5π pulse of Fig. 1(d) at different locations within the waveguide. (b) Calculated temporal profiles of the carrier density N corresponding to those of (a); a_0 is the exciton Bohr radius.

Figures 1(c) and 1(d), corresponding to the experimental results in Figs. 1(a) and 1(b), show the calculated cross-correlations of the transmitted pulses obtained by numerically integrating the coupled semiconductor Maxwell-Bloch equations (1)-(4). Good agreement between theory and experiment is obtained, with pulse breakup clearly evident for the 7.5π pulse in Fig. 1(d).

To obtain physical insight into what is responsible for the observed pulse breakup we have performed an extensive series of diagnostic tests involving the calculated excitation density $N = 2\sum|\psi_\lambda(0)|^2 n_\lambda$ and the pulse shape at different locations ξ within the waveguide. In Fig. 2(a) at $z = \xi = 0 \mu\text{m}$ the excitation density N is seen to closely follow the input intensity with no oscillations. This is consistent with the adiabatic following hypothesis [12], though a residual density remains after the pulse due to the finite polarization dephasing time. Thus the pulse breakup cannot be simply ascribed to off-resonance Rabi oscillations in the excitation density as found in self-induced transparency: The effective Rabi frequency can only decrease with propagation distance since the field amplitude is decaying excluding the possibility of Rabi oscillations downstream. We also note that, in comparison to the work of Grischkowsky, Courtens, and Armstrong in Rb vapor [3], the propagating pulse profile does not show significant pulse steepening. However, the calculations of Figs. 2(a) and 2(b) show that oscillations in the excitation density precede the pulse breakup, and we therefore trace the source of the pulse breakup to the excitation density oscillations. To make this clearer, if we neglect the effects of group-velocity dispersion in Eq. (1), then combining Eqs. (1)-(4) yields the exact result

$$\frac{\partial}{\partial \xi} |\bar{E}(\xi, \eta)|^2 = -\frac{\hbar \mu_0 \omega_0^2}{k_0} \frac{\partial N}{\partial \eta}. \quad (6)$$

So temporal oscillations in N are converted to temporal oscillations in the pulse intensity profile $|\bar{E}(\xi, \eta)|^2$ through propagation, $|\bar{E}(\xi + d\xi, \eta)|^2 - |\bar{E}(\xi, \eta)|^2 \propto \partial N / \partial \eta$.

$$\bar{P}_\lambda(\xi, \eta) = -\frac{id_{cv}}{2\hbar} \int_{-\infty}^{\eta} [1 - 2n_\lambda(\xi, \eta')] \bar{E}(\xi, \eta') e^{i(\omega_\lambda - \omega_0 - 1/\tau)(\eta - \eta')} d\eta'. \quad (7)$$

The coherent nature of the interaction is implicit in the fact that the polarization depends on the prior temporal history of the electric field. Inserting Eq. (7) into Eq. (3) we see that the excitation density n_λ is driven by interference in terms of the form $\bar{E}(\xi, \eta)\bar{E}^*(\xi, \eta')$, between the field at (retarded) time η and earlier times η' . The dominant contributions to these terms come from times obeying $\eta - \eta' < \tau$. For $t_p \gg \tau$, on the other hand, the exponent $\exp[-(\eta - \eta')/\tau]$ becomes strongly damped, the polarization then adiabatically follows the field (time history erased), and the interference terms vanish. Note that this is in perfect accord with our experimental and numerical results for long pulses ($t_p = 5 \text{ ps} \gg \tau = 200 \text{ fs}$) for which pulse breakup was absent. If in the coherent case ($t_p \ll \tau$) the propagating field is sufficiently frequen-

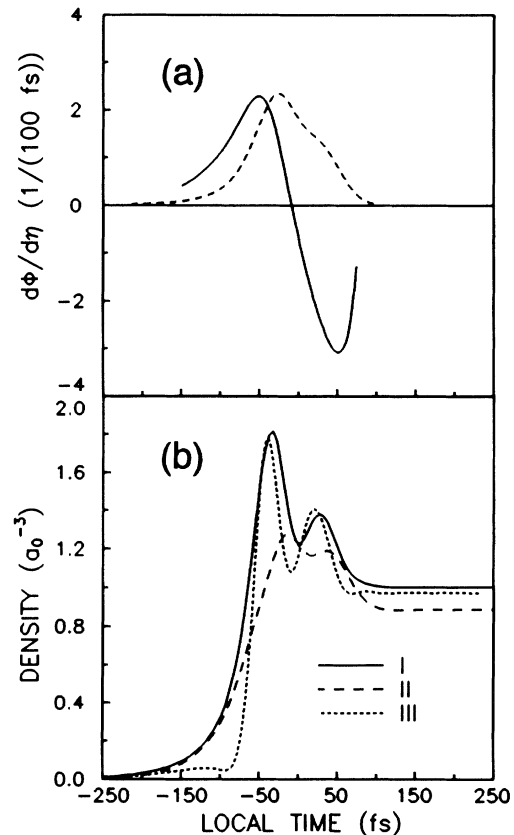


FIG. 3. (a) Calculated frequency chirp $d\phi/d\eta$ (solid line) at $\xi = 120 \mu\text{m}$. The pulse intensity (dashed line) is plotted for reference. (b) Temporal profiles of the carrier density N at $\xi = 120 \mu\text{m}$ resulting from solving the semiconductor Bloch equations with the exact numerical phase solution $\phi(\eta)$ (I, solid line), a first-order fit $\phi(\eta) = \phi_1\eta$ (II, long dashed line), and a second-order fit $\phi(\eta) = \phi_1\eta + \phi_2\eta^2$ (III, short dashed line).

The oscillations in the excitation density which trigger the pulse breakup are due to the coherent light-matter interaction. To see this, one first formally integrates Eq. (2) to obtain

cy chirped by self-phase-modulation, the phase of the electric field changes rapidly enough to escape from the adiabatic following regime and produce interference terms that drive oscillations in the excitation density which in turn cause pulse breakup. To test this mechanism for pulse breakup we have extracted the numerically calculated field at $\xi = 120 \mu\text{m}$, which we write in terms of its real amplitude \mathcal{E} and phase ϕ , $\bar{E}(\xi = 120 \mu\text{m}, \eta) = \mathcal{E}(\eta)\exp[i\phi(\eta)]$. As seen in Fig. 3, while the amplitude $\mathcal{E}(\eta)$ merely shows a small modulation [dashed curve in Fig. 3(a)] the density N [solid curve in Fig. 3(b)] is already oscillating, driven by the large frequency chirp of the instantaneous light frequency, $\Delta\omega(\eta) = -\partial\phi/\partial\eta$. We have also fitted the phase by the

curve $\phi(\eta) \simeq \phi_1\eta + \phi_2\eta^2$ around $\eta=0$, frequency chirping being represented by the second term. Figure 3(b) shows the solution of the semiconductor Bloch equations at $\xi=120 \mu\text{m}$ for the cases (I) exact numerical solution, (II) $\phi(\eta) = \phi_1\eta$, and (III) $\phi(\eta) = \phi_1\eta + \phi_2\eta^2$. It is clear that the approximate simulation including frequency chirping (curve III) is in much better agreement with the exact numerical solution, thus demonstrating that frequency chirping due to self-phase-modulation indeed results in interference terms which drive the excitation density oscillations.

In a Bloch-vector representation one can describe the light-semiconductor interaction at $\xi=0$ by adiabatic following, i.e., the rate of change of \bar{E} ($\simeq 1/100$ fs) is slow compared with the precession frequency $(\Omega^2 + \Delta_{1s}^2)^{1/2}$, and the Bloch vector \mathbf{p} follows the torque vector. But by $\xi=120 \mu\text{m}$, $\partial\phi/\partial\eta$ instantaneously reaches $\Delta_{1s}/2$. This violates the adiabatic following criterion since $\partial\bar{E}/\partial\eta \simeq i(\partial\phi/\partial\eta)\bar{E}$, when $\partial\phi/\partial\eta$ is large [12]. In Bloch-vector jargon the effective field moves too fast for \mathbf{p} to follow; with a component of the effective field perpendicular to \mathbf{p} , \mathbf{p} is rotated giving oscillations in the carrier density N .

In conclusion, we have observed below-resonance, coherent pulse breakup in a room-temperature semiconductor waveguide for the first time. Simulations of the semiconductor Maxwell-Bloch equations identify the effect as propagation-induced escape from adiabatic following. This coherent effect, which is distinctly different from self-induced transparency, a temporal soliton, or self-steepening, should be ubiquitous under off-resonance pulse propagation with a pulse duration less than the polarization dephasing time.

The authors would like to acknowledge support from ARO, NSF, JSOP, NATO travel grant, and the Optical Circuitry Cooperative. One of us, A.K., thanks the Studienstiftung des deutschen Volkes, Germany, for support.

- (a) Also with Faculty of Physics and Astronomy, Institute of Optics and Quantum Electronics, Friedrich-Schiller-University, Max-Wien-Platz 1, O-6900 Jena, Germany.
 (b) Present address: Electrical Engineering Department, Princeton University, Princeton, NJ 08554.
 (c) Also with the Physics Department of the University of Arizona.
- [1] S. L. McCall and E. L. Hahn, *Phys. Rev. Lett.* **18**, 908 (1967); *Phys. Rev.* **183**, 457 (1969).
 [2] R. E. Slusher and H. M. Gibbs, *Phys. Rev. A* **5**, 1634 (1972).
 [3] D. Grischkowsky, E. Courtens, and J. A. Armstrong, *Phys. Rev. Lett.* **31**, 422 (1973).
 [4] P. C. Becker, H. L. Fragnito, C. H. Brito Cruz, R. L. Fork, J. E. Cunningham, J. E. Henry, and C. V. Shank, *Phys. Rev. Lett.* **61**, 1647 (1988).
 [5] K. Watanabe, H. Nakano, A. Honold, and Y. Yamamoto, *Phys. Rev. Lett.* **62**, 2257 (1989).
 [6] D. Fröhlich, A. Nöhte, and K. Reimann, *Phys. Rev. Lett.* **55**, 1335 (1985).
 [7] J. E. Rothenberg and D. Grischkowsky, *Phys. Rev. Lett.* **62**, 531 (1989).
 [8] M. Lindberg and S. W. Koch, *Phys. Rev. B* **38**, 3342 (1988); R. Binder, S. W. Koch, M. Lindberg, N. Peyghambarian, W. Schäfer, and F. Jahnke, *Phys. Rev. Lett.* **65**, 899 (1990).
 [9] W. Rudolph and B. Wilhelmi, *Light Pulse Compression* (Harwood, London, 1989).
 [10] S. G. Lee, P. A. Harten, J. P. Sokoloff, R. Jin, B. Fluegel, K. E. Meissner, C. L. Chuang, R. Binder, S. W. Koch, G. Khitrova, H. M. Gibbs, N. Peyghambarian, J. N. Polky, and G. A. Pubanz, *Phys. Rev. B* **43**, 1719 (1991).
 [11] J. P. van der Ziel and R. A. Logan, *IEEE J. Quantum Electron.* **19**, 164 (1983).
 [12] We take the definition of L. Allen and J. H. Eberly, *Optical Resonance and Two-Level Atoms* (Wiley, New York, 1975), but adiabatic following is also violated in a frame rotating $\omega_0 + \partial\phi/\partial t$ as in Ref. [3]. See D. Grischkowsky, *Phys. Rev. Lett.* **24**, 866 (1970).